

Lithium Insertion in Disordered Carbon–Hydrogen Alloys: Intercalation vs Covalent Binding

P. Papanek, M. Radosavljević,[†] and J. E. Fischer*

Department of Materials Science and Engineering and Laboratory for Research on the Structure of Matter, University of Pennsylvania, Philadelphia, Pennsylvania 19104

Received February 6, 1996. Revised Manuscript Received April 17, 1996⁸

Disordered carbons obtained by pyrolyzing organic solids at $T \leq 700$ °C retain substantial residual hydrogen and exhibit surprisingly large capacities for Li uptake in electrochemical cells. Using semiempirical computer simulations, we show that the high capacity is partially attributable to Li binding on H-terminated edges of hexagonal carbon fragments, with local geometries analogous to the stable isomer of the organolithium molecule $C_2H_2Li_2$. These results can be tested experimentally by vibrational spectroscopy and have implications for further developments in Li-ion rechargeable battery technology.

Introduction

As new materials become more complex, rapid progress toward understanding structure–property relations and optimizing performance relies ever more heavily on close interplay among synthesis, physical characterization, and computer modeling. It is not unusual for the first microscopic insights to come from numerical simulations employing various quantum chemical methods, which in turn point the way to corroborating experiments and improved syntheses. Advances in software and hardware have greatly increased the power and accessibility of computational materials science, to the point that the treatment of complex atomic and molecular systems is now feasible.

The work presented here is such an example. Our goal is to identify the mechanism by which some disordered carbon–hydrogen alloys are able to absorb large amounts of lithium.^{1,2} These have been proposed as alternatives to graphite anodes in rechargeable Li-ion batteries, in which Li ions shuttle back and forth through an electrolyte to “intercalate” either an inorganic oxide or some form of carbon as the battery is discharged or charged, respectively. The benchmark is the graphite intercalation compound LiC_6 in which ordered layers of Li occupy the van der Waals intervals between adjacent graphite monolayers.³ The in-plane Li packing density is restricted by Coulomb repulsion to 4.2 Å, corresponding to the occupation of second-neighbor interstitial sites defined by the hexagonal carbon network. Were it not for this restriction, i.e., if first-neighbor sites could be occupied, the maximum concentration would correspond to LiC_2 , which is in fact accessible by high-pressure synthesis.⁴

The disordered carbons of interest are obtained by pyrolysis of organic precursors at relatively low temperatures. As a result, much of the hydrogen remains, with H/C typically 0.05–0.30.⁵ X-ray diffraction reveals the presence of few-layer graphitic fragments of order 40 Å lateral dimension corresponding to ~20 contiguous hexagons.^{6,7} The location of the residual hydrogen in the technologically relevant materials is not known, but by analogy with amorphous Si:H one expects the H to preferentially saturate the carbon valences on the perimeter of the fragments.^{8,9} There is also little microscopic information about the location of intercalated Li in these materials. Surprisingly, the maximum electrochemical insertion of Li, expressed in battery terminology, can be as high as 1000 mA h/g of carbon; for comparison, crystalline LiC_6 corresponds to 372 mA h/g. An empirical correlation between Li capacity and H concentration suggests a limiting value of one “excess” Li per H,² implying a second reaction path leading to the formation of a bound Li–C–H entity. Alternatively, it has been proposed¹ that Li occupies first-neighbor interstitial sites, i.e., a local motif analogous to high-pressure LiC_2 for which the ideal capacity exceeds 1000 mA h/g. Our computer experiments show that H is intimately involved in Li binding and thus strongly favor the first alternative.

We studied the interactions of Li with C:H alloys by simulating the latter as planar hydrocarbons containing several aromatic rings. Calculations on large systems were performed exclusively at the semiempirical MNDO/AM1 level, the reliability of which was first addressed by comparing AM1 results for smaller molecules with those obtained by ab initio Hartree–Fock and density functional calculations.

[†] Current address: Physics Department, Bates College, Lewiston, ME 04240.

⁸ Abstract published in *Advance ACS Abstracts*, June 1, 1996.

(1) Sato, K.; Noguchi, M.; Demachi, A.; Oki, N.; Endo, M. *Science* **1994**, 264, 556.

(2) Dahn, J. R.; Zheng, T.; Liu, Y.; Xue, J. S. *Science* **1995**, 270, 590.

(3) Guerard, D.; Herold, A. *Carbon* **1975**, 13, 337. Fischer, J. E. in *Chemical Physics of Intercalation*; Legrand, A. P., Flandrois, S., Eds.; Plenum: New York, 1987; p 59.

(4) Avdeev, V. V.; Nalimova, V. A.; Semenenko, K. N. *High Pressure Res.* **1990**, 11, 6.

(5) Zheng, T.; Liu, Y.; Fuller, E. W.; Tseng, S.; von Sacken, U.; Dahn, J. R. *J. Electrochem. Soc.*, to be published.

(6) Liu, Y.; Xue, J. S.; Zheng, T.; Dahn, J. R. *Carbon* **1996**, 34, 193.

(7) The results in ref 6 have been confirmed by P. Zhou of our laboratory using X-ray and neutron radial distribution function analysis.

(8) A variety of C–H bonding environments are observed in different amorphous C:H materials. These show a general tendency for H to saturate π bonds, converting sp^2 to sp^3 carbons: Walters, J. K.; Newport, R. J. *J. Phys. Condens. Matter* **1995**, 7, 1755 and references therein.

(9) Elliott, S. R. *Adv. Phys.* **1989**, 38, 1.

Computational Methods and Test Results

To simplify and consequently speed up the calculations for larger molecules, several semiempirical quantum chemical methods have been developed. These methods usually consider only the valence electrons and require a set of parameters to handle the ionic cores. Additional approximations, such as the zero differential overlap (ZDO) approximation, are made as well. In the MNDO (modified neglect of differential overlap) method¹⁰ the ZDO approximation is applied only to orbitals centered at different atoms. Further improvement of the MNDO method, named AM1,¹¹ was achieved by the modification of core–core repulsion functions and by reparametrization of the fitting functions for the two-center integrals. AM1 is the method of choice especially for conjugated and aromatic systems, for which the calculated geometries are much better than the MNDO results.

The performance of the MNDO Hamiltonian for organolithium compounds was analyzed in several works.^{12,13} In general, qualitatively good results were obtained for many molecules, though the overestimation of the lithium–carbon bond strength (resulting in shorter C–Li bond distances) was also observed, which in some cases leads to less satisfactory geometries. Similar results were found in a recent study by Pratt and Khan.¹⁴

Since lithium has not been parametrized at the AM1 level, we used the older Li parametrization suggested by Thiel¹⁵ and the AM1 parameters for C and H. To check the reliability of this method, we performed several test runs on smaller molecules and compared the AM1 (more precisely Li(MNDO)/AM1) results with ab initio values (which were either previously published or calculated by us). All semiempirical calculations were carried out using the molecular orbital software package MOPAC,¹⁶ and ab initio Hartree–Fock calculations were performed with the Gaussian 94 program.¹⁷ The systems under study exhibit multiple local minima, and a reliable search for the ground state is a problem that can be resolved only by extremely time-consuming techniques such as Monte Carlo or molecular dynamics and simulated annealing. Instead, we tested many different starting configurations and draw conclusions only from those features that are independent thereof. The AM1 calculations were carried out on Sun SPARCstation and Stardent computers (optimization runs of a few minutes for small systems), while the ab initio runs took about 1 CPU hour on Convex C240 and Cray-YMP/C916 computers.

Our first test compound, $C_2H_2Li_2$ in the singlet state, has been recently investigated by ab initio molecular-dynamics simulation based on the Car–Parrinello

method.¹⁸ Starting the AM1 optimization runs from different initial configurations, we obtained results which compare very well with those obtained ab initio. The lowest energy structure denoted as **1** in ref 18 is correctly reproduced as planar, with a linear C–C–H unit bound to a Li_2H triangular complex. The AM1 heat of formation is 13.7 kcal/mol, and the C–C bond distance of 1.216 Å (ab initio value 1.242 Å) suggests an acetylene-like structure. We also optimized the metastable isomers **2–4** and found heats of formation at least 45 kcal/mol higher; in ref 18 the differences are ~35 kcal/mol. The AM1-calculated C–C bond lengths, 1.33–1.37 Å, typical for a double bond, are also in good agreement. The only obvious deficiencies were the C–C–Li bond angles for isomers **2** and **4** which were slightly larger than 90°, whereas the ab initio values are close to 86°.

The performance of the semiempirical method is worse for 1,1-dilithioethylene, $Li_2C=CH_2$. In ab initio studies it was found that the triplet state is more stable than the singlet and that the perpendicular form of the molecule is lower in energy than the planar form.¹⁹ The stabilization of the perpendicular geometry is explained by a strong hyperconjugation of the p orbital on the carbon belonging to the CH_2 group with the two coplanar C–Li bonds. This effect is not sufficiently reflected in the AM1 calculations, although both planar and perpendicular forms could be optimized as stationary states. However, the planar singlet form was more stable than the perpendicular one by about 5.4 kcal/mol. Also, in AM1 the triplet states were always higher in energy than singlets.

Interestingly, the calculated molecular geometries for the singlet states agree within a few percent with the published data; the agreement is better for C–C bonds (e.g., 1.330 Å for the planar form compares well with ab initio 1.347 Å), and slightly worse for C–Li bonds (AM1 1.835 Å, ab initio 1.931 Å). Furthermore, the AM1 method correctly predicts that the C–Li bonds are shorter for the perpendicular species (1.767 Å, ab initio 1.747 Å).

Our next test compound, dilithioacetylene C_2Li_2 , has been shown to possess two stable species: one having fully linear geometry, and a doubly bridged structure with D_{2h} symmetry.²⁰ At the AM1 level both stationary states can be optimized as true local minima, i.e., without any constraints to a particular symmetry. The C–C bond length for the linear molecule is 1.229 Å (ab initio value 1.267 Å) and the C–Li bond is 1.783 Å (ab initio 1.883 Å). For the doubly bridged geometry we obtained C–C distance 1.268 Å (ab initio 1.282 Å) and C–Li 2.005 Å (2.017 Å). Thus, the molecular geometries are calculated quite acceptably. The energy difference between these two structures obtained by AM1 is 15.2 kcal/mol in favor of the linear isomer. A similar result is obtained in ab initio studies with smaller basis sets. This difference decreases if larger basis sets are used (e.g. 5.5 kcal/mol for the 6-31G basis), and at higher levels of theory (when correlation effects are included as well) the doubly bridged structure actually becomes

(10) Dewar, M. J. S.; Thiel, W. *J. Am. Chem. Soc.* **1977**, *99*, 4899.
(11) Dewar, M. J. S.; Zoebish, E. G.; Healy, E. F.; Stewart, J. J. P. *J. Am. Chem. Soc.* **1985**, *107*, 3902.

(12) Kaufmann, E.; Gose, J.; Schleyer, P. v. R. *Organometallics* **1989**, *8*, 2577.

(13) Romesberg, F. E.; Collum, D. B. *J. Am. Chem. Soc.* **1992**, *114*, 2112.

(14) Pratt, L. M.; Khan, I. M. *J. Comput. Chem.* **1995**, *16*, 1067.

(15) Thiel, W. Program MNDOC; Quantum Chemistry Program Exchange, No. 438, **1982**, 2, 63.

(16) Stewart, J. J. P. Program MOPAC 6.0; Quantum Chemistry Program Exchange No. 581.

(17) Frisch, M. J.; et al. Program Gaussian 94, Revision B.1; Gaussian, Inc.: Pittsburgh, PA, 1995.

(18) Rothlisberger, U.; Klein, M. L. *J. Am. Chem. Soc.* **1995**, *117*, 42.

(19) Apeloig, Y.; Schleyer, P. v. R.; Binkley, J. S.; Pople, J. A. *J. Am. Chem. Soc.* **1976**, *98*, 4332.

(20) Schleyer, P. v. R. *J. Phys. Chem.* **1990**, *94*, 5560.

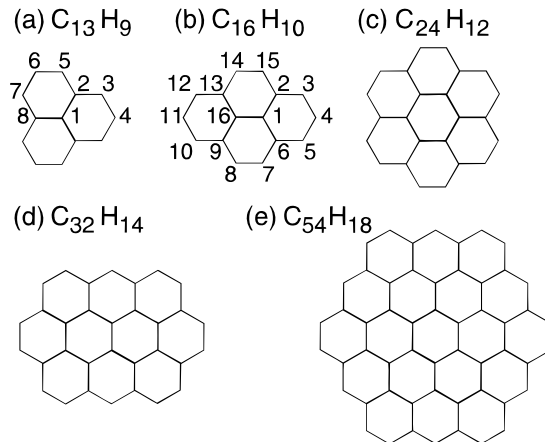


Figure 1. Molecular structures of some of the studied aromatic hydrocarbons. The numbering scheme of C atoms in (a) and (b) is shown for reference in Tables 1 and 2, respectively.

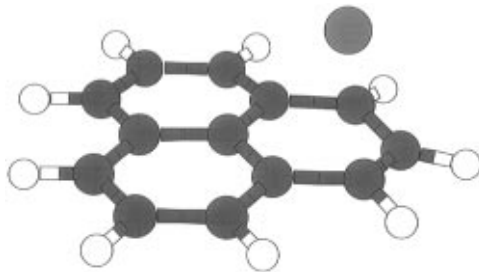


Figure 2. Relaxed structure obtained by adding a single Li to the 3-ring hydrocarbon $C_{13}H_9$; the Li remains in the interstitial position. Results of AM1 and ab initio optimizations are very similar.

more stable by ~ 10 kcal/mole than the linear one. Clearly, the discrepancy between the AM1 and high-level ab initio calculations is largely due to the small basis used in the semiempirical method.

The first aromatic compound, the compact 3-ring hydrocarbon $C_{13}H_9$ (Figure 1a), and its interactions with Li were studied with several techniques. Semiempirical calculations were done with both MNDO and AM1 Hamiltonians to demonstrate the better performance of the latter for aromatic systems. Unrestricted and restricted Hartree–Fock (HF) calculations were carried out using the split-valence 4-31G basis set. The calculations were also repeated within the framework of density functional theory and local spin density approximation (LSDA).²¹

Choosing an initial configuration with the Li over the central carbon, in all calculations the structure relaxes to the geometry shown in Figure 2. The Li is trapped 1.8 Å above a hexagon center, reproducing the normal interstitial position in crystalline LiC_6 . The presence of Li causes a slight distortion from planarity, more pronounced in AM1, due to repulsion between Li and the nearest H.

(21) Here we used one-electron orbitals expanded in Gaussian primitives (Dunlap, B. I.; Connolly, J. W. D.; Sabin, J. R. *J. Chem. Phys.* **1979**, *71*, 3396; Andzelm, J.; Wimmer, E. *J. Chem. Phys.* **1992**, *96*, 1280), and Becke's exchange (Becke, A. D. *Phys. Rev. A* **1988**, *38*, 3098) and Perdew's correlation functionals (Perdew, J. P. *Phys. Rev. B* **1986**, *33*, 8822). The orbital bases for C, H, and Li were at least of double- ζ plus polarization quality and were optimized specifically for use in LSDA calculations (Godbout, N.; Salahub, D. R.; Andzelm, J.; Wimmer, E. *Can. J. Chem.* **1992**, *70*, 560).

Table 1. Interatomic Distances (Å) for $C_{13}H_9$ and $LiC_{13}H_9$ Calculated by Semiempirical and ab Initio Methods^a

	$C_{13}H_9$			
	UHF/MNDO	UHF/AM1	UHF/4-31G	LSDA
C1–C2	1.452	1.429(0)	1.428(8)	1.435
C2–C3	1.434	1.417(1)	1.417(3)	1.422
C3–C4	1.412	1.396(3)	1.394(6)	1.396
	$LiC_{13}H_9$			
	RHF/MNDO	RHF/AM1	RHF/4-31G	LSDA
C1–C2	1.477	1.443	1.441	1.456
C2–C3	1.476	1.445	1.446	1.452
C3–C4	1.425	1.404	1.388	1.412
C2–C5	1.407	1.397	1.387	1.420
C5–C6	1.418	1.402	1.392	1.409
C6–C7	1.387	1.379	1.367	1.396
C7–C8	1.435	1.418	1.412	1.429
C1–C8	1.441	1.425	1.423	1.448
Li···C4	2.208	2.358	2.188	2.254
Li···ring	1.767	1.849	1.828	1.794

^aFor the open-shell molecule $C_{13}H_9$ the unrestricted Hartree–Fock method was applied. The numbering of atoms is shown in Figure 1b, and the Li is located above the hexagon containing C1, C2, C3, C4. Notations A–B and C···D denote atom pairs interpreted as bonded and nonbonded respectively.

The optimized geometries from all simulations with and without Li are summarized in Table 1 (the numbering of atoms is shown in Figure 1a, and Li is centered above the hexagon containing C1, C2, C3, C4). The agreement between the AM1 and Hartree–Fock results is very good, and in general AM1 also performs better than MNDO when compared with LSDA. For AM1, the largest discrepancy in C–C bond lengths is 0.02 Å while the Li–C and Li–ring distances are overestimated by ~ 0.1 Å. All calculations reproduce the observed expansion of C–C bonds nearest to the Li.³ Fitting the electrostatic potential to partial atomic charges gives $Li^{0.588+}$ from LSDA, and the Mulliken population analysis gives $Li^{0.593+}$ from AM1, and $Li^{0.597+}$ from RHF/4-31G.

We note that a second stable minimum for the $LiC_{13}H_9$ system exists, in which the Li is between the two nearest hydrogens of different rings and above the molecular plane. On the other hand, we found it impossible to stabilize 2 Li's over first-neighbor hexagons on the same side of the molecule. Starting the Li's on opposite sides produced stable structures whose features are common to the larger systems as discussed in the next section.

We conclude that the AM1 method is quite reliable in identifying (at least qualitatively) the stable local minima of organolithium systems. It suffers from some deficiencies because steric repulsions are overestimated and the basis set is small. The potential energy of the torsion of CLi_2 group is also handled badly. This should not pose a problem in our calculations, however, as we do not expect the presence of such groups in the systems investigated here.

Interactions of Li with Small Aromatic Hydrocarbons

In the previous test molecule $C_{13}H_9$, all three hexagons are terminated with three hydrogens. In contrast, the hexagons in the 4-ring hydrocarbon $C_{16}H_{10}$ (pyrene) are terminated by either two or three hydrogens (cf. Figure 1b), referred to as "2H" and "3H". In our AM1

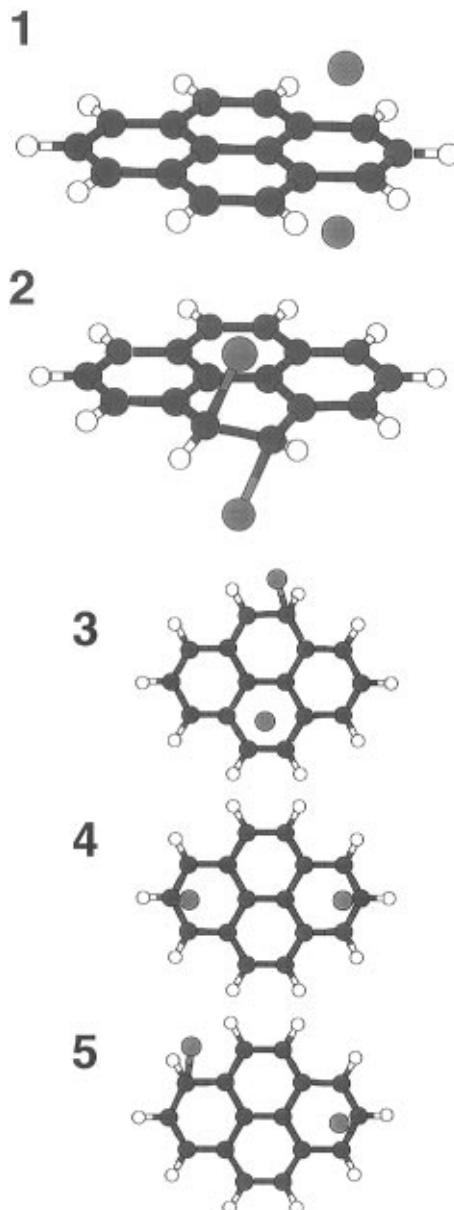


Figure 3. AM1-relaxed structures obtained by adding two Li's to the 4-ring hydrocarbon $C_{16}H_{10}$ in various starting configurations. **1** and **2**, shown in perspective in (a), result from initial Li positions on opposite sides of the molecule centered over 3H and 2H rings, respectively. **3–5**, shown in plan view in (b), are obtained with initial positions on the same side of the molecule (see text). In contrast to Figure 2, here we find evidence for Li bonding via formation of sp^3 -hybridized carbons on the periphery.

calculations we find local minima with a single Li approximately centered above 2H (heat of formation 88.7 kcal/mol) or 3H ($\Delta H_f = 85.3$ kcal/mol), consistent with the three-ring result, and also expected from the analogy with intercalated graphite. However, adding Li in pairs to give “ $Li_2C_{16}H_{10}$ ” produced interesting differences depending on whether they started out above and below a 3H or a 2H ring. The results are shown in Figure 3a; we label these structures **1** and **2**, respectively. Starting from 3H, the relaxed geometry **1** maintains the interstitial Li positions with about 2 Å between the Li's and the molecular plane (8% greater than the experimental value for LiC_6 ³). On the other hand, starting from 2H (which would be degenerate with 3H in an infinite sheet), both Li's move off the interstitial sites and bond to the two peripheral carbons to form

Table 2. Interatomic Distances (Å) for Structures 1 (Interstitial) and 2 (Bonded) of $Li_2C_{16}H_{10}$, Optimized by Restricted Hartree–Fock Calculations Using the 4-31G Basis Set^a

struct 1	struct 2
C1–C2	1.430
C2–C3	1.503
C3–C4	1.399
C6–C7	1.404
C7–C8	1.363
C8–C9	1.425
C9–C10	1.400
C10–C11	1.380
C9–C16	1.423
C1–C16	1.426
Li1…C2	2.220
Li2…C6	2.220
C1–C2	1.398
C2–C3	1.410
C3–C4	1.365
C4–C5	1.397
C5–C6	1.393
C6–C7	1.452
C7–C8	1.540
C1–C6	1.439
C2–C15	1.434
C14–C15	1.342
C1–C16	1.454
Li1–C8	2.035
Li2–C7	2.035

^aBoth isomers possess the C_2 symmetry, although no symmetry restrictions were applied in the optimization.

2. This requires sp^3 hybridization of both carbons so the conjugation of that particular aromatic ring is destroyed, an effect referred to as 1,2-bis-localization.²² The sp^3 character is reflected in the greatly increased bond length, 1.52 Å between the two carbons. The (Li,H) environment in **2** corresponds almost identically to ab initio isomer **2** of $C_2H_2Li_2$, which in fact is the lowest energy isomer compatible with a carbon ring structure.¹⁸

To verify these results, we repeated the calculations at the ab initio level using the 4-31G basis set. The optimized geometries are very similar to those shown in Figure 3a, although now the “doped” 3H ring in **1** and 2H in **2** are even more distorted from planarity (such that, e.g., the structure **1** does not possess mirror symmetry but only a C_2 axis). Furthermore, the Li's are moved slightly off center, so that in **1** one lithium is closest to carbon C2 and the second to C6 (the numbering scheme is shown in Figure 1b). The bond lengths for both structures are summarized in Table 2. We stress that for the bonded isomer **2** the relevant C–C bond length is 1.54 Å, again typical of a single bond.

The energy difference between **1** and **2** calculated by AM1 is very small, **2** being only 0.4 kcal/mol higher than **1**. However, the relative energies are reversed in the HF results, where in fact the bonded configuration is 6.3 kcal/mol (~0.27 eV) *lower* in energy. If the energy difference between interstitial and bonded lithium is similar in real materials, then at higher Li concentration (when the average Li–Li distance is smaller) such local bonded configurations involving the sp^3 hybridization of peripheral carbons should be quite abundant.

The different character of Li–pyrene interaction for the interstitial and bonded configuration was also confirmed by a vibrational analysis performed at the AM1 level. In particular, the infrared (IR) active Li–ring stretching mode occurs at 542 cm^{−1} in **1**, whereas the IR active Li–C stretching vibration in **2** is calculated at 559 cm^{−1} (i.e., 17 cm^{−1} blue-shifted). These numbers suggest that the energy hypersurface is shallower near the local minimum for the interstitial complex.

On the basis of ⁷Li NMR spectra of a heavily Li-doped carbon with H/C = 0.24, it has been suggested that Li_2 molecules are first formed above the plane of the

(22) Dewar, M. J. S.; Dougherty, R. C. *The PMO Theory of Organic Chemistry*; Plenum: New York, 1975; p 149.

Table 3. Heats of Formation (kcal/mol) and Interatomic Distances (Å) for Some AM1 Local Minima of $\text{Li}_2\text{C}_{16}\text{H}_{10}^a$

struct	ΔH_f	Li…Li	Li…C	Li–C	$\text{C}_{\text{Li}}-\text{C}_{\text{Li}}$	$\text{C}_{\text{Li}}-\text{C}_\text{H}$	$\text{C}_{\text{Li}}-\text{C}_\text{Z}$
1	99.8	4.047	2.388				
2	100.2	4.200		2.057	1.521		1.444
3	114.1	5.204	2.420	2.018		1.472	1.446
4	96.7	5.615	2.307				
5	95.5	6.059	2.320	2.078		1.437	1.462
6	93.4	6.609	2.336				

^a In the fourth and fifth columns we distinguish between unbonded (…) and bonded (–) Li/C neighbors. For **2**, the sixth column gives the “single-bond” length between sp^3 -hybridized carbons to which Li’s and H’s are bonded. Similarly for **3** and **5**, the seventh column gives the length of the bonds between the sp^3 carbon to which Li and H is bonded and the sp^2 carbon to which only H is bonded. The distances in the last column are between Li-bonded carbons and the nearest carbon which forms an apex with an unperturbed ring.

graphene sheets, with Li–Li distance ~ 2.7 Å.¹ We have therefore optimized several structures with two Li’s on the same side of the pyrene molecule. Structures **3–5**, shown in Figure 3b, relaxed from initial conditions with both Li’s above two first-neighbor 2H’s, two 3H’s, and a first-neighbor 2H–3H pair, respectively. Our first deduction is that Li–Li repulsion is too strong for stable occupation of first-neighbor sites regardless of starting configuration. We also note the possibility of binding a single Li to either a 2H or 3H ring (structures **3** and **5**, respectively), while the 3H rings refused to bind 2 Li’s starting from opposite sides of the molecule. We believe that edge carbons on 2H rings are more likely to become sp^3 -hybridized than 3H because this preserves conjugation over a larger area of the molecule; two Li’s bonded to a 3H ring would destroy aromaticity (or ring conjugation) of several neighboring rings. On this basis, adding three Li’s to the same 3H ring would be equivalent to two Li’s on a 2H, but the additional electrostatic repulsion would increase the energy of such a structure.

The lowest ΔH_f for $\text{Li}_2\text{C}_{16}\text{H}_{10}$ was obtained for structure **6** (not shown) which is similar to **4** but with (distorted) interstitials on opposite sides of the molecule. Energies and some of the interatomic distances are summarized in Table 3, which is by no means exhaustive; there are many other local minima within a few kcal/mol of the listed values. The systematic progression of energies and Li–Li distances for **3–5** shows that stability is governed mainly by Li–Li interactions. The least stable is **3** with the shortest Li–Li distance in a single layer, shorter Li–Li distances occurring only when the Li’s are on opposite sides (**1** and **2**) such that the ionic repulsion is screened by the pyrene. Similarly, **6** is particularly stable due to the combination of screening and a very large Li–Li distance.

An appreciable volume fraction of the materials of interest consists of few-layer stacks of hexagonal carbon sheets. These were simulated by adding three Li’s to a sandwich of two pyrenes. The resulting structures were entirely analogous to those for a single molecule; starting a column of three Li’s centered on 3H rings preserves the interstitial geometry, while a 2H initial configuration gives two bonded and one interstitial Li. Energies are not reliable due to the poor representation of intermolecular interactions in AM1.

The compact 7-ring hydrocarbon coronene consists entirely of 2H hexagons (Figure 1c). Starting a single Li in any conceivable position always produces a stable

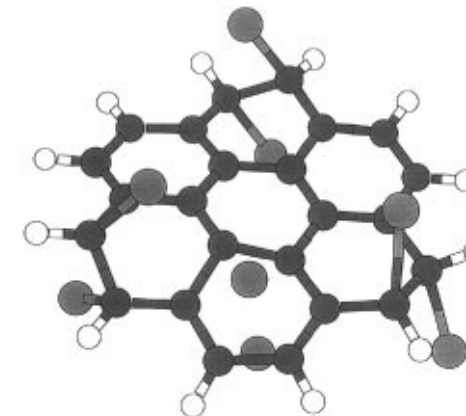


Figure 4. Metastable configuration of $\text{Li}_8\text{C}_{24}\text{H}_{12}$. Six Li atoms are bonded to alternating peripheral rings, and the additional two are stabilized in the interstitial positions above and below another peripheral ring. The molecular plane is significantly distorted from planarity.

Li interstitial. On the other hand, adding **2** on both sides of a hexagon failed to stabilize interstitials. We thought the outcome would be prejudiced in favor of interstitial Li by starting one above and one below the central hexagon; surprisingly, they migrated together to an edge and formed single bonds with neighboring peripheral carbons, as above. A particularly stable configuration with six Li’s consisted of the now familiar “ $\text{C}_2\text{H}_2\text{Li}_2$ ” configurations on alternating peripheral rings, all the lithiums bonding to sp^3 -hybridized carbons. When two additional Li’s were added above and below the central hexagon, the system relaxed to the configuration shown in Figure 4. Whereas six Li’s remained bonded, the additional two are stabilized in interstitial positions above and below one of the *peripheral* rings. The resulting apparent “first-neighbor” Li occupancy in one part of the molecule can be explained by a combination of two effects: (1) partial charges of the interstitial lithiums are appreciably smaller (0.30, compared to 0.49 for the bonded Li’s), which means that the lower energy levels of the coronene molecule are filled, the charge transfer is smaller, and the electrostatic repulsion between Li’s is reduced; (2) the repulsion between Li ions is also significantly *screened* by the π -orbitals of the C–C bonds common to both nearest hexagons because of the large out-of-plane deformation of the molecule. Indeed, if we consider for example two Li ions “fixed” in the interstitial positions above the centers of two fused hexagons, which are then bent downward about the shared C–C bond, then not only the Li–Li distance is larger, but also the lobes of the π -orbitals fill the volume between the ions to a greater extent. We found similar screening effects in larger systems, leading to deformed and curved graphene sheets, which will be discussed in the following section. In Figure 4, due to the deformation of the molecule and the fact that the bonded Li’s are away from ring centers, the shortest Li–Li distance is more than 2.91 Å.

We note that the $\text{Li}_8\text{C}_{24}\text{H}_{12}$ configuration corresponds to the highest Li:C ratio for which the lithium still binds to the molecule. Introducing additional Li’s resulted in forming Li_2 and larger Li clusters. The clusters are not completely neutral; the calculated charge on a lithium in cluster usually ranged from ~ 0.06 to 0.24. Also, the clusters usually migrated toward the edges, and their distance from the molecular sheet was greater than the

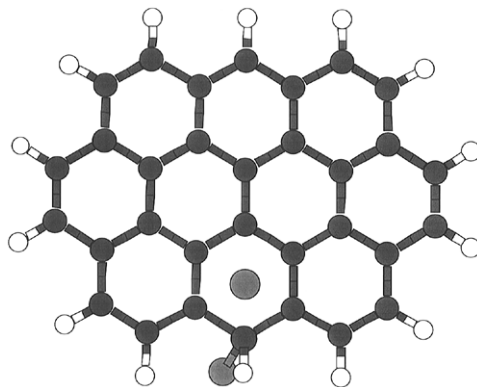


Figure 5. Structure of $\text{Li}_2\text{C}_{32}\text{H}_{14}$ with one interstitial Li above the 1H ring, and second Li bonded to the peripheral carbon.

distance of bonded or interstitial Li's. We interpret these results as the "saturation" limit for the molecule to form stable (or metastable) compounds with Li, which in the real electrode material would correspond to maximum Li uptake capacity.

AM1 Calculations for Larger Systems

We will now briefly summarize some of the most interesting results of our AM1 calculations performed for larger systems (>40 atoms). The aromatic hydrocarbon ovalene $\text{C}_{32}\text{H}_{14}$ is a particularly good representative of a graphene sheet as it also contains the one-hydrogen terminated hexagons (1H) and the inner hexagons (Figure 1d). Local minima exist with one interstitial lithium above any of the aromatic rings. Whereas the energies of configurations with an interstitial Li above a 2H ring or above a 1H ring are almost identical, the structure with one Li above an inner hexagon is higher in energy by ~ 6.5 kcal/mol. When additional lithiums were introduced we observed similar tendencies as for the smaller molecules, and the total energy was again determined mainly by the Li–Li separation.

As before, if two lithium atoms happen to be on different sides of the molecule near a 2H ring, sp^3 hybridization takes place and C–Li bonds are formed. Contrary to the results for coronene, the $\text{Li}_2\text{C}_{32}\text{H}_{14}$ system also has a stable local minimum with two interstitial Li's above and below one of the inner hexagons. This shows that the interaction between lithium and planar hydrocarbons is greatly influenced by the topology of a particular graphene-like sheet.

Another interesting result is that two Li's cannot be stabilized in the interstitial position above and below a 1H ring of the $\text{C}_{32}\text{H}_{14}$ molecule. Instead, the AM1 optimization produces a configuration with one lithium in the interstitial site above the molecular plane, while the second Li below the plane is pushed away from the ring center and closer to hydrogens, albeit within a bonding distance to the peripheral carbon (C–Li distance 2.06 Å, Figure 5). The local environment of this carbon is now suggestive of sp^3 hybridization (C–C bond length 1.49 Å), and also the hydrogen atom of the 1H ring is significantly displaced above the plane, so that the carbon appears to be almost tetrahedrally coordinated. We have seen such local configurations in a number of optimization runs for different aromatic hydrocarbons; nevertheless, it cannot be generalized as a universal feature of the 1H peripheral hexagons. In

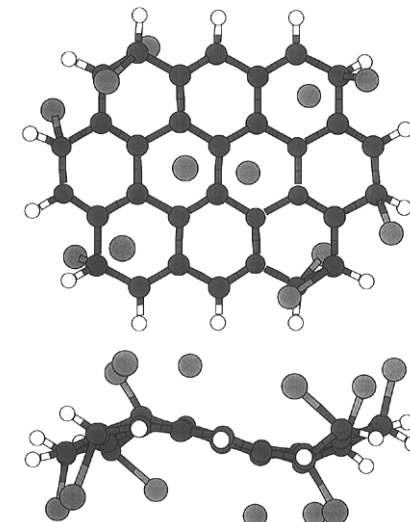


Figure 6. Top and side views of a particular configuration of the $\text{C}_{32}\text{H}_{14}$ molecule doped with 12 lithiums. Nearest-neighbor Li's are observed above or below the 2H and inner rings, and the molecular sheet is strongly deformed.

some molecular geometries (mainly nonalternant aromatic hydrocarbons for which the classical single- and double-bond structure cannot be drawn) the 1H rings stabilize two Li's in the "normal" interstitial configuration, which again illustrates the richness of the behavior of Li-doped aromatic systems.

In making analogies between intercalated graphite and doped disordered carbon, it is often overlooked how flexible the graphene sheets are, especially along the [100] (graphite) directions. We demonstrate this using as an example a particular configuration of $\text{Li}_{12}\text{C}_{32}\text{H}_{14}$, shown in Figure 6. As can be seen in the side view, the molecular sheet is significantly deformed as a result of the doping. Such deformations are especially pronounced in systems with partial nearest-neighbor Li occupancy. The shortest Li–Li distance in the configuration shown is 3.09 Å between the Li atoms above the 2H and inner rings. The two central Li's are on different sides of the molecule such that the structure has inversion symmetry. We should mention that in the simulation the doping was carried out in several steps by optimizing intermediate structures with smaller numbers of lithiums, and with no symmetry constraints. It was also necessary to introduce new Li atoms in positions sufficiently separated from other Li's, because in the AM1 optimization the immediate formation of covalently bonded Li clusters significantly decreases the total energy of the heavily doped systems. Dynamically, however, such a process would require surmounting a potential barrier of order ~ 100 kcal/mol due to Coulomb repulsion between Li's, which in fact leave the electrolyte as Li^+ ions in the real system.

The hexagonal shaped molecule $\text{C}_{54}\text{H}_{18}$ (Figure 1e) was the largest single sheet considered in this work. We have focused mainly on the possibility to stabilize nearest-neighbor Li interstitials of the inner hexagons; however, we were not able to find any such metastable structure. Initial configurations with Li in nearest-neighbor sites relax quickly to structures with larger Li–Li separation, and when lithium is judiciously introduced in Li_2 clusters, these are displaced away from the molecular plane.

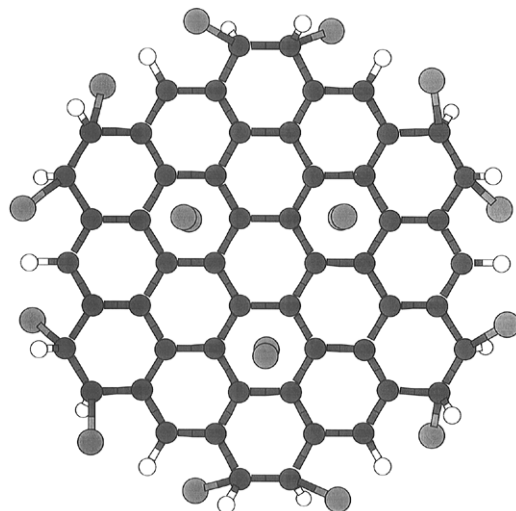


Figure 7. AM1-optimized structure of $\text{Li}_{18}\text{C}_{54}\text{H}_{18}$ with 12 bonded Li atoms at the molecular perimeter and six Li's in the second-nearest-neighbor interstitial sites.

Our attempts to relax a stable $\text{Li}_{14}\text{C}_{54}\text{H}_{18}$ configuration with second-nearest-neighbor Li site occupancy above and below the central aromatic ring and all 1H rings resulted in a disordered structure comprising both interstitial and bonded Li's. As in previous results the 2H rings display a high affinity for the bonded configuration, and the behavior of 1H rings is similar as in the $\text{C}_{32}\text{H}_{14}$ compound. Therefore, the $\text{Li}_{14}\text{C}_{54}\text{H}_{18}$ isomer with 12 Li's bonded to 2H rings and 2 Li's above and below the central hexagon can be easily optimized, although it is not the energetically most favorable structure. We note that for systems of this size even the semiempirical optimization run takes of the order of 10 CPU hours (Stardent) so that the search for the global minimum is a very time-consuming task.

The structure shown in Figure 7 is a $\text{Li}_{18}\text{C}_{54}\text{H}_{18}$ isomer with all Li's bound to the molecule, six of them being in the typical second-neighbor interstitial sites and the remaining 12 bonded to the 2H hexagons. The observed “wider” bonded configuration corresponds to the familiar one shown in pyrene (**2** in Figure 3a) after twisting the LiCH species by about 180° . In the depicted structure such configuration is energetically more favorable since it increases the nearest Li–Li distance between a bonded and interstitial lithium. This result also demonstrates that the AM1 technique is able to predict the second-neighbor arrangement of interstitial Li's characteristic of the LiC_6 graphite intercalation compound. However, the total C/Li ratio is 3:1 because of the Li bonding at the molecular perimeter.

In fact, the C/Li ratio is about the same also for larger structures with similar arrangement of Li atoms. With increasing size, the number of interstitial Li's (proportional to the area of the sheet) increases faster than the number of bonded Li's at the periphery (which is proportional to the circumference), and the stoichiometry approaches LiC_3 because there are two second-nearest-neighbor Li layers for a single graphene sheet. In the bulk, such assumption of two Li layers sandwiching a single carbon layer requires significant separation between sandwiches. Furthermore, our calculations show that a structure with two Li layers between two parallel $\text{C}_{54}\text{H}_{18}$ sheets is not stable, implying that the graphitic layers have to be arranged in a *nonparallel*

fashion to allow lithium occupation on both sides of a single layer. This brings us to the “house of cards” proposal to explain the high Li capacity in hard carbons² which also have much smaller hydrogen content. In these materials, the Li–C–H bonding mechanism probably plays a less significant role.

Conclusions

The results of our semiempirical optimizations strongly suggest that residual hydrogen in low-T pyrolyzed disordered carbons provides a second mechanism for Li uptake which operates in parallel with the well-known intercalation of Li into interstitial sites. This provides a natural explanation for the large reversible Li capacity exhibited by these materials. Since ab initio calculations also predict the Li–C bonding, the semiempirical results can be accepted with some confidence.

The bonding of inserted lithium at the edges of H-terminated graphene sheets also involves changes in the nature of bonding between the peripheral carbons. Such bonding changes in the host material have been shown to cause a hysteresis in electrochemical measurements, i.e., the dopant ions are inserted and removed at different voltages.²³ We note that a large hysteresis (approximately 1 V) is exhibited especially by those materials which contain a substantial amount of hydrogen.² Recently, it has been proposed that this hysteresis is the result of different activation energies for Li hopping between two interstitial sites compared to Li hopping between a bonded and a interstitial site.²⁴

In most of our calculations the total energies for the bonded and intercalated structures are very similar; the differences are on the order of a small fraction of an eV per inserted Li, although they also depend on the topology of a particular aromatic hydrocarbon molecule. Tacitly assuming that our gas-phase results also hold in the bulk solid, we may expect that both mechanisms occur at nearly the same potential in a battery and both contribute to the reversible Li capacity. Our preliminary vibrational analysis of some of the Li-doped systems shows that several of the vibrational modes are significantly shifted if Li–C bonds are formed. In situ spectroscopic experiments performed during electrochemical doping might be able to identify the onset of the bonding regime by observing changes in the low-frequency spectra (both Li–C and Li–ring stretching vibrations seem to occur below 600 cm^{-1}). We also expect that useful information can be provided by inelastic neutron-scattering experiments, especially for the materials with high hydrogen content, because of the large incoherent cross section of the proton. The presence of $>\text{CHLi}$ species should be readily detectable because of their twisting and rocking vibrations, which can be well resolved using the filter-analyzer technique.²⁵

In several optimization runs for systems with Li/C ratio $\approx 1/3$ we have observed nearest-neighbor arrangement of Li ions, though in most cases only on one side of the molecule. A common feature of such metastable configurations was a greatly deformed and curved

(23) Selwyn, L. S.; McKinnon, W. R.; von Sacken, U.; Jones, C. A. *Solid State Ionics* **1987**, 22, 337.

(24) Dahn, J. R., private communication.

(25) Papanek, P.; Fischer, J. E.; Sauvajol, J. L.; Dianoux, A. J.; Mao, G.; Winokur, M. J.; Karasz, F. E. *Phys. Rev. B* **1994**, 50, 15668.

molecular plane. We believe that the screening effect of π -electrons at places where the graphene sheet is bent plays an important role in reducing the Coulomb repulsion between Li ions. Admittedly, it is necessary to investigate this phenomenon at a higher level of theory.

In the AM1 calculations the ratio $\text{Li/C} \approx 1/3$ appears to be the highest achievable doping concentration, which translated to the electrochemical cell capacity would correspond to $\sim 740 \text{ mA h/g}$. Values in this range are typical for low-T pyrolyzed soft carbons and represent the upper limit of Li capacity for the hard carbon electrode materials with high H content. The latter consist primarily of small single carbon layers arranged roughly like a "house of cards", and it has been proposed that single sheets bind a layer of lithium on both sides also in the bulk if there is appreciable nanoporosity in the material.²

To reproduce the huge Li uptake capacity (almost 1000 mA h/g) for H-rich soft carbons which consist of few-layer stacks of sheets, it is probably necessary to include additional features in the model calculations. Obviously, several graphene sheets have to be considered, but the presence of unsaturated "dangling" bonds at the sheet perimeter could play an even more impor-

tant role in stabilizing the excess lithium. Another phenomenon worth further study is the presence of disclinations in the hexagonal network (caused by 5- and 7-membered rings) and their effect on the character of interaction between Li and the curved sheet.

Global minima and other properties of Li-doped carbons and hydrocarbons can be studied further by using the AM1 energies and gradients as input to molecular dynamics and simulated annealing. The good correspondence between AM1 and ab initio results for these systems implies that further rapid progress in organolithium chemistry can be made with the less-demanding semiempirical simulations as a useful starting point.

Acknowledgment. Principal support for this work was provided by the National Science Foundation MRL Program under Grant DMR91-20668. Supercomputer resources were provided by the Department of Energy under Grant DE-FC02-86ER45254. We are grateful to M. L. Klein for useful discussions.

CM960100X